

# TIQA: Human-Aligned Text Quality Assessment in Generated Images

Kirill Koltsov<sup>1</sup> Aleksandr Gushchin<sup>2,3,1</sup> Dmitry Vatolin<sup>2,3,1</sup> Anastasia Antsiferova<sup>2,3,4</sup>

## Abstract

Text rendering remains a persistent failure mode of modern text-to-image models (T2I), yet existing evaluations rely on OCR correctness or VLM-based judging procedures that are poorly aligned with perceptual text artifacts. We introduce Text-in-Image Quality Assessment (TIQA), a task that predicts a scalar quality score that matches human judgments of rendered-text fidelity within cropped text regions. We release two MOS-labeled datasets: TIQA-Crops (10k text crops) and TIQA-Images (1,500 images), spanning 20+ T2I models, including proprietary ones. We also propose ANTIQA, a lightweight method with text-specific biases, and show that it improves correlation with human scores over OCR confidence, VLM judges, and generic NR-IQA metrics by at least  $\sim 0.05$  on TIQA-Crops and  $\sim 0.08$  on TIQA-Images, as measured by PLCC. Finally, we show that TIQA models are valuable in downstream tasks: for example, selecting the best-of-5 generations with ANTIQA improves human-rated text quality by +14% on average, demonstrating practical value for filtering and reranking in generation pipelines.

## 1. Introduction

The rapid development of generative AI has made AI-generated images widely accessible, with text-to-image (T2I) systems becoming simultaneously faster, cheaper, and higher quality. Recent models have improved substantially on prompt semantics and global realism, as reflected in modern benchmarks (UC Berkeley, n.d.; Li et al., 2024; Zhang et al., 2025b). Yet *text rendering* remains a persistent failure mode: generated images often exhibit malformed glyphs, broken strokes, inconsistent thickness, and unstable kerning or baselines (Figure 1). These errors are highly salient in

<sup>1</sup>Lomonosov Moscow State University, Moscow, Russia <sup>2</sup>ISP RAS Research Center for Trusted Artificial Intelligence, Moscow, Russia <sup>3</sup>MSU Institute for Artificial Intelligence, Moscow, Russia <sup>4</sup>Innopolis University, Innopolis, Russia. Correspondence to: Aleksandr Gushchin <alexander.gushchin@graphics.cs.msu.ru>.

Preprint. March 10, 2026.



Figure 1. Examples of text rendering artifacts in AI-generated images across multiple generators. Even when text remains partially readable, humans penalize visual artifacts. TIQA is the task of assessing these perceptual failures rather than semantic correctness.

practical, text-heavy outputs (posters, UI mockups, pseudo-documents), but current evaluations lack a dedicated way to measure the *perceptual fidelity* of rendered text.

Existing approaches typically evaluate text in images either through recognition-centric pipelines (e.g., OCR against ground-truth text) or by using a large vision-language model (VLM) as a general-purpose judge. Both are useful, but neither reliably captures perceptual text quality. OCR-based scores primarily reflect semantic correctness and require ground truth; they can under-penalize appearance defects that humans judge harshly (e.g., stroke breaks, irregular thickness, kerning/baseline instability) even when the string remains decodable. VLMs can, in principle, reason about such artifacts across languages and styles, but practical use of VLMs as a benchmark signal faces well-known obstacles: (i) the output is the result of a prompting/decoding procedure and is sensitive to prompt wording, sampling, and preprocessing, making standardization difficult (Gu et al., 2024; Zhu et al., 2024); (ii) closed, frequently updated APIs introduce version drift, so benchmark outcomes can change over time without changes to the evaluated method; and (iii) even in adjacent perceptual-quality tasks, specialized quality models can outperform GPT-4V-style judges despite detailed instructions (You et al., 2024; 2025). Together, these limitations motivate a dedicated model that directly targets perceptual text artifacts.

We address this gap by introducing *Text-in-Image Quality Assessment* (TIQA): predicting a scalar score for a detected text region that matches human judgments of rendered-text fidelity, *independent of semantic correctness*. The main contributions of this work are as follows:

- **New task formulation (TIQA).** We introduce *text-in-image quality assessment* (TIQA): given a detected text region in an AI-generated image, the goal is predict a single perceptual quality score aligned with human judgments of rendering artifacts (e.g., malformed glyphs, broken strokes, character hallucinations), *independent of the semantic correctness of the text*.
- **Two datasets for benchmarking and training.** **TIQA-Crops** contains 120k OCR-detected text crops generated by 12 T2I models, including 10k crops with MOS labels and 110k additional crops used for proxy-supervised pretraining via OCR confidence. **TIQA-Images** provides 1,500 full-frame, text-heavy images from 10 recent generators (e.g., GPT Image 1.5, Nano Banana Pro), each paired with a text-only view and dual MOS annotations (overall and text-only). We will make these datasets public.
- **Method (ANTIQA).** We develop ANTIQA, a specialized TIQA model that outperforms strong baselines, including OCR-derived confidence, generic IQA metrics, and VLM-based judges, under both in-distribution and cross-generator evaluations. We observe improvements in correlations over the second-best method across all settings (e.g., +0.08 PLCC for the latest T2I models).
- **Analysis and applications.** We characterize text rendering failures across modern T2I systems (including proprietary models) and quantify remaining gaps; we also demonstrate that TIQA scores enable effective filtering/best-of- $K$  selection and are useful in downstream vision-language tasks on text-heavy images.

## 2. Related Work

We study no-reference, crop-level prediction of perceptual text rendering quality in AI-generated images, targeting typographic artifacts (glyph topology/shape, stroke continuity/thickness, etc.) rather than semantic string correctness.

**Improving text rendering in generative models.** Rendered text can be improved via text-aware conditioning, layout/glyph guidance, and post-editing/inpainting pipelines (Tuo et al., 2023; Chen et al., 2023a; Shimoda et al., 2025). These methods benefit from reliable local feedback to train, guide, or rerank generations. TIQA provides this missing signal with a MOS-aligned, region-level score for typographic appearance that is independent of semantic correct-

ness, complementing OCR-based correctness metrics and prompted-judge approaches.

**Image quality evaluation and AIGC evaluation.** Image generators are commonly evaluated with distributional realism metrics (IS (Salimans et al., 2016), FID (Heusel et al., 2017)) and, when references exist, full-reference fidelity (PSNR/SSIM, LPIPS (Zhang et al., 2018)). In the no-reference setting, generic IQA spans blind-feature models (BRISQUE (Mittal et al., 2012)), learned MOS predictors (NIMA (Talebi & Milanfar, 2018)), and transformer-based methods (TOPIQ (Chen et al., 2024a)). Preference/reward/judge scores (e.g., (Xu et al., 2023; Kirstain et al., 2023)) assess semantic match, aesthetics, or overall quality, but they are not designed to isolate fine-grained text rendering artifacts that can dominate human judgments in text-heavy images while leaving global realism largely unchanged.

**Evaluating text in AI-generated images: correctness vs. appearance.** Text evaluation for T2I outputs is often recognition-centric: OCR outputs are compared to prompts or ground truth (e.g., (Fallah et al., 2025; Zhang et al., 2025a)) using CER/Levenshtein metrics. While effective for decodability and semantic match, such measures can underpenalize perceptual defects (broken strokes, malformed glyph topology, unstable kerning/baselines) that humans rate poorly even when text is readable. VLM/LLM-based judging procedures (e.g., (Bosheah & Bilicki, 2025; Sampaio et al., 2024)) are more holistic, but the score is the outcome of a procedure (prompting, decoding, preprocessing, cropping) rather than a standardized metric, and it can be sensitive to prompt wording and model/version drift, consistent with broader “LLM-as-a-judge” findings (Gu et al., 2024; Zhu et al., 2024; You et al., 2024; 2025). These issues are amplified in region-level text crops, where small preprocessing differences can alter perceived artifacts.

**Downstream use and adjacent text-centric IQA.** Learned scorers are increasingly used to curate data (Schuhmann et al., 2022), rank and selection of best-of- $K$  samples (Kirstain et al., 2023; Xu et al., 2023), and provide reward signals for refinement (Lee et al., 2023; Eyring et al., 2024; Xu et al., 2023). Yet these workflows typically rely on generic IQA, prompt-alignment scorers, or correctness proxies (OCR confidence/string match), which are poorly matched to typographic failure modes. Adjacent document/screen-content IQA and text legibility works (Ye & Doermann, 2013; Min et al., 2021; Colombo et al., 1987) address physical degradations (blur/compression) but not characteristic generative failures (hallucinated strokes, inconsistent glyph topology, style-inconsistent character formation), nor a MOS-aligned signal calibrated to typographic plausibility in AI-generated text. TIQA complements these directions by focusing on generative artifacts in detected text regions.

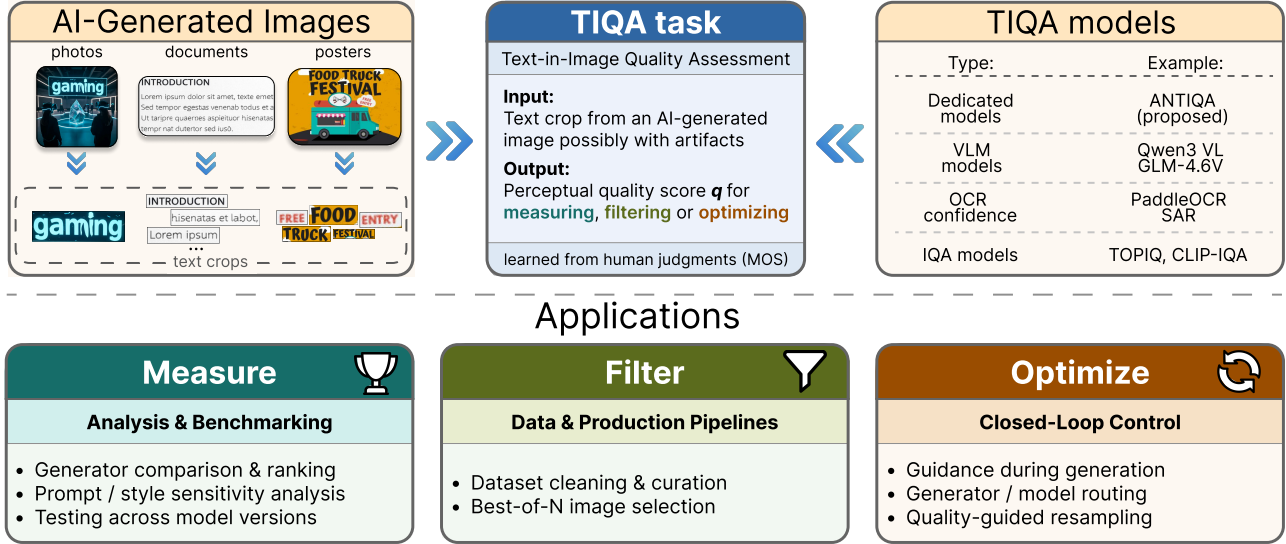


Figure 2. Overview of Text-in-Image Quality Assessment (TIQA). Left: AI-generated images contain multiple text regions that are detected and cropped. Middle: a TIQA model predicts a scalar text-quality score for each crop, trained on mean opinion scores (MOS). Right: representative model families used as baselines (VLM judges, OCR confidence, generic IQA) and the proposed specialized TIQA model. Bottom: example applications of TIQA for measuring generator quality, filtering candidates in production pipelines (best-of-K), and optimizing generation via reranking or closed-loop control.

### 3. Text-in-Image Quality Assessment (TIQA) for AI images

We introduce *Text-in-Image Quality Assessment* (TIQA): given a detected text crop (a cropped image region containing rendered text), predict a scalar perceptual quality score learned from human judgments. Figure 2 summarizes the task, representative model families, and downstream uses for measuring, filtering, and optimizing text-in-image generation.

#### 3.1. Task definition

We propose text-in-image quality assessment (TIQA), a specialization of no-reference image quality assessment (IQA) for rendered text. Classical IQA aims to predict how an image appears to humans under common distortions (e.g., blur, noise, compression). In contrast, TIQA focuses on generator-induced text artifacts that corrupt the appearance of text in AI-generated images. Crucially, TIQA is *independent of semantic correctness*: it evaluates how the text is rendered, not what the text says. Thus, a semantically correct string with perceptual rendering artifacts (e.g., malformed glyphs, broken strokes) must receive a lower TIQA score than a visually clean but misspelled string.

Formally, given a text crop  $x \in \mathcal{X} \subseteq \mathbb{R}^{H \times W \times 3}$ , TIQA predicts a scalar score  $f(x) \in \mathbb{R}$  that correlates with the mean opinion score (MOS)  $s(x)$  of rendered-text quality. We learn  $f$  by minimizing the expected loss function  $\ell$

$$\min_f \mathbb{E}_{x \sim \mathcal{X}} [\ell(f(x), s(x))], \quad (1)$$

where  $s(x)$  reflects the severity of AI-specific text artifacts rather than classical camera/codec degradations. For text crops, such artifacts primarily violate: (i) glyph integrity (character topology and stroke continuity), (ii) typographic regularity (spacing, alignment, baselines, consistent font style), and (iii) scene binding (physically consistent compositing on surfaces, perspective, and illumination). Examples of text crops with artifacts are shown in Figure 1. Additional examples are provided in Appendix C.3.

We propose evaluating the TIQA model performance using standard correlation metrics on MOS-annotated datasets: Pearson’s Linear Correlation Coefficient (PLCC) and Spearman’s Rank Order Correlation Coefficient (SROCC).

#### 3.2. Downstream Tasks

Beyond benchmarking, TIQA models provide a control signal that can be used throughout text-heavy generation pipelines: for data curation, as guidance during training or sampling, and at inference time for filtering and quality-aware routing of OCR/VLM reasoning when outcomes depend on rendered text. We highlight four representative use cases:

1. **Reranking and filtering:** Rank multiple candidates per prompt by predicted text quality, or apply accept/reject thresholds. If all candidates fall below a threshold, resample up to a fixed budget and return the best obtained, reducing illegible or visually corrupted text without changing the base generator.

2. **Quality-aware routing for OCR/VLM reasoning:** When synthetic artifacts (malformed glyphs, inconsistent strokes, broken spacing, hallucinated characters) cause OCR/VLM failures, TIQA can (i) gate OCR outputs (accept vs. abstain), (ii) trigger re-generation/re-rendering (e.g., new seed/typography/layout), and (iii) pre-check text-dependent VQA to abstain or fall back to OCR-assisted reasoning when text is unlikely to be reliable.
3. **Guidance for T2I models:** Use TIQA as a reward for selection among samples, or as an auxiliary objective during sampling/training to improve rendered text while keeping prompt semantics fixed.
4. **Data curation for training:** Filter or stratify text-containing samples for OCR/VLM training to remove severe degradations, control difficulty (curricula or balanced sampling), and reduce noisy supervision from incoherent text.

We evaluate reranking in Section 6.3 and the ability of AN-TIQA to predict failures of OCR and VLM vision tasks in App. B.1.

## 4. Datasets for TIQA

For training and analysis, we propose two datasets: **TIQA-Crops** and **TIQA-Images**. TIQA-Crops contains 120,000 cropped text regions extracted from 36,000 AI-generated images produced by a diverse set of 12 T2I models. We annotate 110,000 crops with OCR confidence and use them only for the pretraining procedure. The remaining 10,000 crops are annotated with MOS of perceptual text quality, enabling supervised training and in-domain evaluation.

We additionally introduce TIQA-Images, a dataset designed to analyze TIQA behavior and characterize modern T2I models on text-heavy prompts. Unlike TIQA-Crops, which provides localized text-region crops, TIQA-Images consists of full-frame images (the entire generated image, without cropping). It contains 1,500 images generated by 10 T2I models, including proprietary systems (e.g., Nano Banana Pro, GPT Image 1.5), each annotated with two image-level MOSes: overall quality and text-only quality (Section 4.2). For both datasets, each element is annotated with at least 50 ratings; details are below.

### 4.1. TIQA-Crops dataset: training and in-domain evaluation

**Data Collection.** We used a prompt dataset from TextInVision (Fallah et al., 2025) to construct a large-scale, diverse dataset of AI-generated text artifacts in images. The dataset provides 50,000+ methodically designed text-in-image prompts spanning simple, complex, and real-world

scenarios (e.g., ads and educational materials), with prompt complexity and text attributes independently varied. The text strings are grouped into single words, phrases, and long multi-sentence text, with controlled difficulty (Oxford 5,000 CEFR A1–C1) and stress cases such as gibberish, misspellings, numbers, and special characters.

We sampled 3,000 prompts from the TextInVision (Fallah et al., 2025) dataset and generated 36,000 AI images using 12 T2I models. From the resulting images, we extracted 120,000 text regions using the PP-OCRv5 (Cui et al., 2025) text detection model. The resulting crops include both clean text and diverse generation-induced text artifacts. More details about the prompts, the list of T2I models, and examples of the final crops are provided in Appendix C.

**Human Annotation.** To collect subjective quality scores, we used the Yandex.Tasks platform (Yandex, n.d.). We designed a 0–5 text-quality scale, where 0 indicates no text, and 5 indicates ideal quality. Participants were instructed to evaluate *visual artifacts in the rendered text*, while *ignoring meaning or spelling as much as possible*, since these aspects can be evaluated by OCR and VLM models. To guide raters, we provided detailed instructions, descriptions, and visual examples for each score from 0 to 5.

To be eligible to participate, subjects had to pass an exam consisting of 10 questions with evenly distributed ground-truth scores and answer at least 8 questions correctly. We also filtered low-quality responses with verification questions. In total, for 10,000 text crops, we collected 500,000+ scores from ~4,500 unique participants. For the full instructions, statistics, and other details, see Appendix D.

### 4.2. TIQA-Images: Text-Heavy Images from Modern T2I Models

To complement our crop-level training data, we introduce **TIQA-Images**, a text-heavy benchmark of full AI-generated images. TIQA-Images is designed to analyze (i) how well TIQA models generalize to *unseen* generators and prompts, and (ii) how overall image quality relates to the perceptual quality of rendered text. To help disentangle text artifacts from surrounding visual content, we additionally construct a paired text-only view for each image (described below).

**Image generation.** We created a set of 30 text-heavy prompts that reliably produce challenging typography (e.g., dense layouts, small fonts, mixed font styles, long paragraphs, numbers, and structured text such as lists or pseudo-documents). We rendered each prompt with 10 recent text-to-image generators via `replicate.com`, including GPT Image 1.5, Nano Banana Pro, Flux 2 [max], SeeDream 4.5, etc. For each (model, prompt) pair, we generated 5 images using different random seeds, resulting in total 1500 images.

**Text-only rendering.** For each image, we derive a text-only

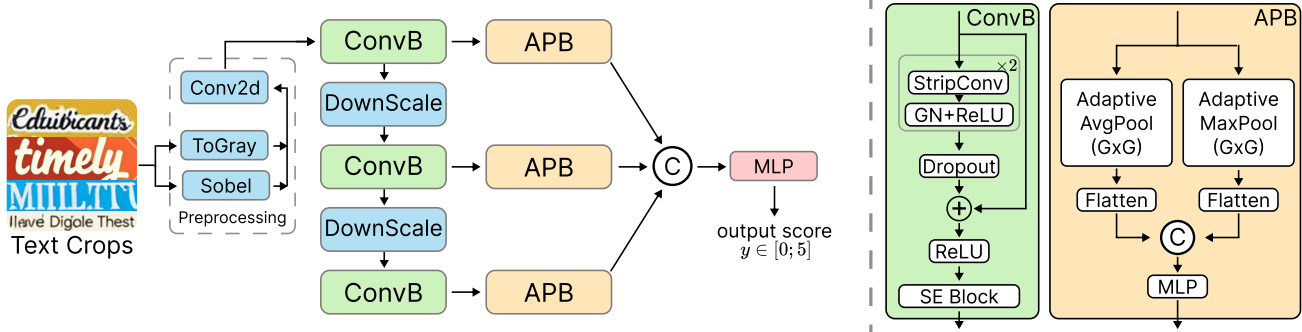


Figure 3. ANTIQA architecture. Each text crop is converted to grayscale, concatenated with a Sobel edge map, and then processed by a lightweight multi-scale CNN with residual stages and downsampling. Features from multiple resolutions are pooled to fixed grids using adaptive average and max pooling, fused via an MLP head, and regressed to a single MOS prediction.

version that preserves the rendered text while removing surrounding content. Concretely, we detect text regions using PP-OCRv5 (Cui et al., 2025) and construct a binary mask; pixels outside the mask are set to a uniform white background, while pixels inside the text regions are preserved exactly. This isolates the text’s perceptual quality from non-textual visual factors.

**Subjective study protocol.** We collect human judgments under two complementary rating tasks, each using an integer 0–5 scale (higher is better), and compute the mean opinion score (MOS) as the mean rating across raters:

(i) **Overall quality (OQ-MOS; full-frame image).** Raters score the overall perceptual quality of the complete image, considering any visible degradations (e.g., blur, noise, geometry issues, and text artifacts).

(ii) **Text quality (TQ-MOS; text-only).** Raters score only the *perceptual quality of the text*, using the corresponding text-only image. They are instructed to ignore semantics (meaning, correctness, or sense of the written content) and judge only visual artifacts such as malformed glyphs, broken strokes, character substitutions, spacing/kerning issues, and inconsistent baselines. The two tasks are run independently, yielding paired MOS annotations for overall image quality and text-only quality.

Full list of used T2I models and their parameters, examples of images from the datasets, curated list of prompts for TIQA-Images, and subjective instructions can be found in App. C. We also evaluate participants’ ability to separate visual quality from semantics (App. D.1).

## 5. Method: ANTIQA

We design the architecture and training procedure with the following criteria in mind: (i) the model must capture fine-grained glyph details and global word-level structure; (ii) the model should be robust across fonts/styles/generators; (iii) the model should be fast enough for large-scale use.

### 5.1. Architecture

As shown in Figure 3, ANTIQA predicts a single MOS score from a text crop represented by a 2-channel input (grayscale concatenated with a Sobel edge map). The model is a compact multi-scale CNN regressor composed of repeated **ConvB** stages with two **DownScale** transitions, followed by per-scale **APB** pooling and a fusion head.

**ConvB: directional strip residual blocks with SE.** A core design choice is to use residual *strip* convolutions ( $1 \times k$  and  $k \times 1$ ) inside each **ConvB** stage. This injects an anisotropic inductive bias that matches text geometry: glyph strokes, stems, and baselines are elongated structures whose degradations (broken strokes, ringing/aliasing, baseline jitter, uneven spacing) often manifest more strongly along one axis. In our implementation (Figure 3, right), each **ConvB** applies two strip-convolution layers with GroupNorm+ReLU, followed by Dropout and a residual skip connection, then a ReLU. A final SE block (*squeeze-and-excitation*, Hu et al. 2018) performs lightweight channel-wise recalibration: global spatial “squeeze” aggregates each channel to a scalar, a small gating MLP computes per-channel importance weights, and the resulting “excitation” scales feature channels to emphasize informative responses and suppress nuisance variations (e.g., font/style differences), improving robustness with minimal overhead.

**APB: multi-scale pooling and fusion.** ANTIQA extracts features at three resolutions and applies an Adaptive Pooling Block (APB) at each scale. As shown in Figure 3, **APB** performs adaptive average pooling and adaptive max pooling to a fixed  $G \times G$  grid, flattens each pooled tensor, concatenates the two descriptors, and projects them with a small per-scale MLP. The three per-scale embeddings are then concatenated (operator  $C$  in the figure) and passed to a final MLP to predict the MOS score.

ANTIQA contains 3.8M parameters and requires 31.5 GFLOPs per  $256 \times 256$  crop, enabling efficient evaluation.

## 5.2. Training

We first pretrain ANTIQA on 110k text crops without MOS scores using OCR confidence scores from PP-OCRv5 model mapped to the MOS range. The OCR confidence→MOS mapping is computed via neural optimal transport (Korotin et al., 2022), aligning the proxy-score distribution to the MOS distribution while preserving monotonicity in practice. To compute the mapping function we used only the training part of the TIQA-Crops. These 110k crops are disjoint (by image ID) from the 10k MOS-labeled crops. We then finetune on 10,000 MOS-labeled crops from TIQA-Crops dataset with a mixed objective combining MSE and pairwise ordering:  $\mathcal{L} = \mathcal{L}_{\text{MSE}} + \lambda \mathcal{L}_{\text{rank}}$ , where  $\mathcal{L}_{\text{rank}}$  is:

$$\mathcal{L}_{\text{rank}} = \frac{1}{|B|} \sum_{i < j} [\text{softplus}(-\text{sign}(y_i - y_j)(\hat{y}_i - \hat{y}_j))], \quad (2)$$

where  $y$  denotes MOS value,  $\hat{y}$  is predicted score, and  $|B|$  is the size of a mini-batch. This encourages both calibrated scores and correct relative preferences, matching correlation-based evaluation. Architecture and training details for ANTIQA are provided in Appendix A.1. We ablate ANTIQA’s design choices in Appendix B.4.

## 6. Experiments

### 6.1. Experimental Setup

For evaluation, we employ two widely used correlation coefficients for MOS-annotated quality assessment: Pearson’s Linear Correlation Coefficient (PLCC) and Spearman’s Rank Order Correlation Coefficient (SROCC).

To prevent leakage from near-duplicate crops, we split TIQA-Crops by source image ID (all crops from the same image are assigned to the same split). We report results only on the held-out test split. This way, the 10,000 MOS-annotated crops from TIQA-Crops were split into training (9,000), validation (500), and test (500) sets. TIQA-Images was used in its entirety without further splitting.

We compare against three baseline families: (i) OCR confidence scores: PaddleOCR 3.0 (Cui et al., 2025), SAR (Li et al., 2019); (ii) VLM-based judges: Qwen3 (Yang et al., 2025), GLM 4.6 (Zhipu AI (Z.ai) Model Team, 2025); and (iii) a generic no-reference IQA metric TOPIQ (Chen et al., 2024a). For VLM judges, we prompt the model to score text rendering fidelity only on a 0-5 scale (floats allowed), ignoring textual meaning/spelling; the score is the first parsed number. Additional details on model selection and VLM prompting are provided in Appendix A.

**Image-level aggregation for TIQA-Images dataset.** We aggregate crop scores into an image-level score via area-

weighted pooling:

$$Q_{\text{ANTIQA}}(x) = \frac{\sum_{i=1}^N w_i q(c_i)}{\sum_{i=1}^N w_i}, \quad w_i = \text{area}(c_i), \quad (3)$$

where  $c_i$  denotes a text crop from image  $x$ ,  $N$  is the number of text crops in  $x$  and  $q(c_i)$  is model’s predicted quality for crop  $c_i$ . We also report an ablation of alternative pooling strategies in Appendix A.4.

### 6.2. Results on TIQA-Crops

Table 1 summarizes correlation coefficients on the TIQA-Crops dataset for ANTIQA and other baseline models. On TIQA-Crops, ANTIQA outperforms OCR confidence and VLM judges on crop-level MOS, indicating that recognizing text is not sufficient: the model must also capture visual degradations specific to rendered glyphs (e.g., stroke breaks, bleeding, aliasing). The relatively strong Qwen3 crop performance suggests VLMs can judge local text when text occupies most pixels, but this advantage does not directly transfer to full-image scoring on TIQA-Images. VLM models are also computationally heavy, with an average FPS of 0.6 for Qwen3. In contrast, the generic NR-IQA baseline TOPIQ performs substantially worse than text-specific signals, indicating that general-purpose IQA metrics do not adequately capture rendered-text quality.

### 6.3. Results on TIQA-Images

We evaluate whether a dedicated text-in-image quality assessor (ANTIQA) better matches human judgments than generic image-quality evaluation methods on *unseen* modern text-heavy T2I outputs. None of the 10 generative models represented in TIQA-Images was used during ANTIQA training. As described in Section 4.2, TIQA-Images dataset contains OQ-MOS and TQ-MOS for each image, corresponding to overall and text quality, respectively.

Crop-based methods (ANTIQA, OCR) operate on detected text regions and are pooled to image-level, as described in Eq. 3; full-frame baselines (TOPIQ, VLM judges) score the entire image for Table 1. We also evaluate VLM judges under three different computation modes in Table 2.

#### **ANTIQA generalizes well to unseen SOTA generators.**

We also evaluate overall alignment with humans across all 1,500 images by reporting SROCC and PLCC between method scores and MOS values. Table 1 reports global correlations on the TIQA-Images dataset for both overall and text-only MOS values (OQ-MOS and TQ-MOS, respectively), where ANTIQA achieves the strongest correlation with both TQ-MOS and OQ-MOS. It is important to note that TIQA-Images contains images from T2I models that were not seen during ANTIQA training, making it well-generalizable to new SOTA generators.

Table 1. Performance on TIQA-Crops (crop-level) and TIQA-Images (image-level) measured by PLCC/SROCC with human MOS. Higher is better. Best is bolded, second-best is underlined.

Type	Model	TIQA-Crops		TIQA-Images (OQ-MOS)		TIQA-Images (TQ-MOS)		Speed (FPS)
		PLCC $\uparrow$	SROCC $\uparrow$	PLCC $\uparrow$	SROCC $\uparrow$	PLCC $\uparrow$	SROCC $\uparrow$	
IQA	TOPIQ	0.401	0.414	0.615	0.568	0.493	0.470	56.8
OCR	PaddleOCR	0.778	0.788	<u>0.671</u>	<u>0.664</u>	<u>0.761</u>	<u>0.787</u>	<b>133.3</b>
	SAR	0.690	0.709	<u>0.569</u>	0.591	0.634	0.640	19.1
VLM	Qwen3	<u>0.891</u>	<u>0.921</u>	0.471	0.443	0.447	0.424	0.6
	GLM 4.6	0.674	0.671	0.257	0.343	0.193	0.288	0.4
TIQA	ANTIQA (ours)	<b>0.942</b>	<b>0.935</b>	<b>0.810</b>	<b>0.797</b>	<b>0.842</b>	<b>0.837</b>	<u>119.0</u>

**VLM judging is localization-sensitive.** Table 2 also reveals that VLM judges are substantially stronger when we restrict their input to the text region. On full images, rendered text often occupies a small fraction of pixels, and the model’s judgment can be dominated by non-text content, diluting sensitivity to glyph-level artifacts. Using the text-only masked view (marked by \*) reduces this context leakage by suppressing non-text regions, improving alignment with TQ-MOS. Evaluating the VLM per detected text crop and averaging across crops (marked by \*\*) further boosts performance by (i) effectively zooming in to preserve stroke-level details and (ii) reducing variance by aggregating multiple local judgments into a stable image-level score.

**Text and overall quality scores are strongly coupled.** We observe a strong association between human overall quality (OQ-MOS) and text quality (TQ-MOS) on TIQA-Images (SROCC on the whole dataset is  $\approx 0.78$ ). To verify that this is not purely an “across-generator” effect, we decompose the correlation by the dataset hierarchy (Table 4 in Appendix). Across generator-level averages (10 groups), the correlation is near-perfect (PLCC=0.96, SROCC=0.98). More importantly, when holding the generator and prompt fixed and varying only the random seed (5 images per (generator,prompt)), the within-group association remains strongly positive (mean SROCC=0.51, median=0.59). Together, these results show that the OQ-TQ coupling is not merely driven by differences between generators but persists within fixed generator–prompt settings, implying that in this text-heavy regime overall preference is largely constrained by text rendering failure, which is consistent with a text-specialized signal outperforming generic NR-IQA on OQ-MOS despite being trained for text quality.

**ANTIQA excels at best-of- $K$  selection.** To test whether a method can identify the best sample among multiple generations of the *same* prompt and generator, we evaluate ranking performance on each group of  $K=5$  images from the TIQA-Images dataset. Each group of images corresponds to one (prompt, generator) pair and contains  $K=5$  images. For every group, we compute the correlation between predicted

quality scores and MOS across the  $K$  samples, and then average over all  $S=300$  groups. We report results for both TQ-MOS and OQ-MOS, which is especially challenging in this text-heavy regime because small within-group differences must be detected across only  $K=5$  samples.

Table 2 shows that ANTIQA achieves the strongest within-group agreement with human rankings for both TQ-MOS (PLCC/SROCC: 0.419/0.382) and OQ-MOS (0.388/0.340). In contrast, generic NR-IQA (e.g., TOPIQ) correlates better with OQ than TQ, consistent with IQA emphasizing global naturalness and artifacts rather than text legibility. OCR confidence (PaddleOCR) is competitive for text ranking (0.415/0.364) but transfers poorly to overall quality (0.171/0.165), indicating that recognizing text is not sufficient to capture visual preference. VLM-based scorers underperform on both criteria, suggesting limited calibration for fine-grained, within-prompt comparisons.

**Best-of- $K$  selection improves human MOS.** Correlation captures ranking consistency, but in practice, we aim to select the best sample based on quality. For each (prompt, generator) group, we choose the image with the highest predicted quality score produced by a given method and report its average MOS:

$$\text{MOS}^\dagger = \frac{1}{S} \sum_{i=1}^S \text{MOS}\left(s_i^{k_i^*}\right), k_i^* = \arg \max_{k \in \{1, \dots, K\}} q_i^{(k)} \quad (4)$$

where  $\{s_i^1, \dots, s_i^K\}$  is the set of  $K$  samples in group  $i$ , and  $q_i^k$  is the corresponding predicted score output by the evaluated method. The selected index  $k_i^*$  corresponds to the sample that the method predicts to be best within group  $s_i$ .

As shown in Table 2, ANTIQA yields the largest MOS gains over Random selection: +0.36 on TQ-MOS (2.57  $\rightarrow$  2.93, 14% improvement) and +0.30 on OQ-MOS (3.01  $\rightarrow$  3.31, 9.9% improvement), closing **72%** and **65.2%** of the gap to an Oracle selector, respectively. Notably, PaddleOCR improves TQ-MOS substantially (+0.34) but provides only a modest OQ-MOS gain (+0.14), reinforcing that OCR con-

Table 2. Best-of- $K$  ranking/ selection on TIQA-Images. Within-group PLCC/SROCC to MOS are averaged over groups (mean $\pm$ std). Selection reports the mean MOS of the top-scored image per group and  $\Delta$  over Random. Gap closed is computed as improvement over Random relative to Oracle. Random is averaged over 1,000 runs; Oracle is target-specific (max TQ-MOS for TQ, max OQ-MOS for OQ).

Type	Model	Within-group correlation to MOS (mean (std)) $\uparrow$				Best-of-5 selection outcome (mean MOS / gain)			
		TQ-MOS		OQ-MOS		Selected MOS		$\Delta$ MOS vs Random (gap closed)	
		PLCC	SROCC	PLCC	SROCC	TQ	OQ	TQ	OQ
Reference	Random	—	—	—	—	2.57	3.01	+0.00 (0%)	+0.00 (0%)
	Oracle	—	—	—	—	3.07	3.47	+0.50 (100%)	+0.46 (100%)
IQA	TOPIQ	0.115 (0.247)	0.096 (0.251)	<u>0.296 (0.225)</u>	<u>0.280 (0.230)</u>	2.71	3.14	+0.14 (28%)	+0.13 (28.3%)
OCR	PaddleOCR	<u>0.415 (0.232)</u>	<u>0.364 (0.234)</u>	0.171 (0.261)	0.165 (0.262)	<u>2.91</u>	<u>3.15</u>	<u>+0.34 (68%)</u>	<u>+0.14 (30.4%)</u>
	SAR	0.325 (0.245)	0.319 (0.231)	0.120 (0.267)	0.116 (0.259)	2.81	3.08	+0.24 (48%)	+0.07 (15.2%)
VLM	Qwen3	0.060 (0.276)	0.049 (0.271)	0.099 (0.263)	0.122 (0.256)	2.68	3.08	+0.11 (22%)	+0.07 (14.1%)
	Qwen3*	0.181 (0.240)	0.162 (0.229)	0.131 (0.258)	0.125 (0.249)	2.75	3.12	+0.18 (36%)	+0.11 (22.8%)
	Qwen3**	0.265 (0.229)	0.249 (0.221)	0.219 (0.257)	0.211 (0.246)	2.81	3.13	+0.24 (48%)	+0.12 (26.1%)
	GLM 4.6	0.027 (0.267)	0.026 (0.257)	0.067 (0.253)	0.052 (0.249)	2.66	3.06	+0.09 (18%)	+0.05 (10.9%)
	GLM 4.6*	0.148 (0.251)	0.136 (0.249)	0.112 (0.253)	0.102 (0.251)	2.74	3.10	+0.17 (35%)	+0.09 (18.5%)
	GLM 4.6**	0.185 (0.249)	0.174 (0.247)	0.136 (0.255)	0.142 (0.254)	2.76	3.12	+0.19 (38%)	+0.11 (23.9%)
TIQA	ANTIQA	<b>0.419 (0.212)</b>	<b>0.382 (0.211)</b>	<b>0.388 (0.230)</b>	<b>0.340 (0.235)</b>	<b>2.93</b>	<b>3.31</b>	<b>+0.36 (72%)</b>	<b>+0.30 (65.2%)</b>

fidence captures legibility but misses broader factors that drive overall human preference. In summary, ANTIQA consistently selects higher-MOS images, making it a strong drop-in signal for generation-time filtering and reranking when prompts and generators are held fixed. We also evaluate the ability of ANTIQA to predict failures of OCR and VLM vision tasks in App. B.1.

#### 6.4. Text quality comparison of the latest T2I models

TIQA-Images dataset was also used to investigate the quality of text generation of latest T2I models. As described in Section 4.2 we collect MOS scores for text-only version of AI images. Figure 4 presents box-plots for distributions of both MOS values for each generator. We observe a clear improvement in text rendering from older baselines (e.g., SDXL) to the newest models. However, for every generator OQ consistently exceeds TQ, indicating that visual plausibility systematically overstates text fidelity: images can look convincing while the embedded text remains degraded. Robustness remains the primary limitation—TQ distribu-

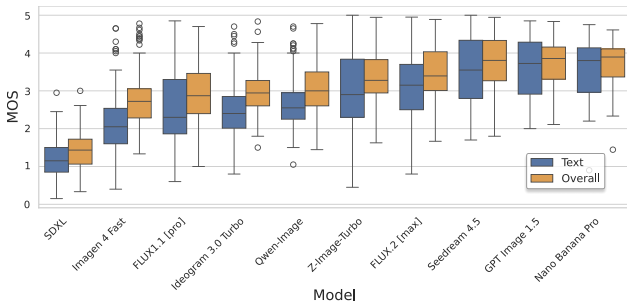


Figure 4. Box-plot distributions of OQ-MOS and TQ-MOS for separate generators. The models are sorted by mean TQ-MOS.

tions exhibit low-score outliers across models, reflecting rare but severe failures and strong sensitivity to prompts and rendering conditions. Consequently, when text correctness is critical, tail behavior is more informative than central tendency (e.g., the median).

## 7. Conclusion

This paper introduces Text-in-Image Quality Assessment (TIQA), a no-reference task for predicting a scalar, MOS-aligned perceptual score of rendered-text fidelity in AI-generated images targeting perceptual text artifacts rather than semantic correctness. We release two benchmarks: TIQA-Crops (120k OCR-detected crops with 10k MOS labels and 110k proxy-labeled crops spanning 12 T2I models) and TIQA-Images (1,500 text-heavy full images from 10 recent generators with paired overall and text-only MOS). We also propose ANTIQA, a lightweight, text-biased multi-scale CNN that achieves the strongest alignment with human judgments across settings (e.g., PLCC 0.942 on TIQA-Crops and PLCC 0.842/0.810 on TIQA-Images for text-only/overall MOS), while remaining efficient for large-scale deployment. Importantly, ANTIQA scores are directly useful in practice: best-of-5 reranking with ANTIQA improves human-rated text quality by +0.36 MOS ( $\approx 14\%$ ) and overall quality by +0.30 MOS, demonstrating value for filtering and selection in generation pipelines. Our analysis further shows that, on text-heavy prompts, text quality strongly drives overall preference, and despite clear progress in modern generators, text rendering remains a persistent bottleneck with notable tail failures—motivating future work on integrating TIQA signals into closed-loop guidance/training and broader coverage of real-world typography.

## Impact Statement

This paper presents work whose goal is to advance the field of Machine Learning. There are many potential societal consequences of our work, none of which we feel must be specifically highlighted here.

## References

- AI, S. Deepfloyd if (if-i-m and related checkpoints), 2022a. URL <https://stability.ai/news/deepfloyd-if-text-to-image-model>. Model card.
- AI, S. Stable diffusion v2.1, 2022b. URL <https://huggingface.co/qualcomm/Stable-Diffusion-v2.1>. Model card. Accessed: 2026-01-29.
- AI, S. Stable diffusion 3.5 large, 2024a. URL <https://huggingface.co/stabilityai/stable-diffusion-3.5-large>. Model card. Accessed: 2026-01-29.
- AI, S. Stable diffusion 3.5 large turbo, 2024b. URL <https://huggingface.co/stabilityai/stable-diffusion-3.5-large-turbo>. Model card / release. Accessed: 2026-01-29.
- AI, S. Stable diffusion 3 medium, 2024c. URL <https://huggingface.co/stabilityai/stable-diffusion-3-medium>. Model card / release. Accessed: 2026-01-29.
- AI, S. Stable diffusion 3 medium (announcement), 2024d. URL <https://stability.ai/news/stable-diffusion-3-medium>. Blog / release. Accessed: 2026-01-29.
- Alibaba, Q. T. . Qwen-image (model repo / release), 2025. URL <https://github.com/QwenLM/Qwen-Image>. Model repo / release. Accessed: 2026-01-29.
- Bosheah, Z. and Bilicki, V. Challenges in generating accurate text in images: A benchmark for text-to-image models on specialized content. *Applied Sciences*, 15(5): 2274, 2025.
- Chen, C., Mo, J., Hou, J., Wu, H., Liao, L., Sun, W., Yan, Q., and Lin, W. Topiq: A top-down approach from semantics to distortions for image quality assessment. *IEEE Transactions on Image Processing*, 33:2404–2418, 2024a. doi: 10.1109/TIP.2024.3378466. URL <https://doi.org/10.1109/TIP.2024.3378466>.
- Chen, J., Huang, Y., Lv, T., Cui, L., Chen, Q., and Wei, F. Textdiffuser: Diffusion models as text painters. *Advances in Neural Information Processing Systems*, 36: 9353–9387, 2023a.
- Chen, J., Yu, J., Ge, C., Yao, L., Xie, E., Wu, Y., Wang, Z., Kwok, J., Luo, P., Lu, H., and Li, Z. Pixart- $\alpha$ : Fast training of diffusion transformer for photorealistic text-to-image synthesis, 2023b. URL <https://arxiv.org/abs/2310.00426>. arXiv preprint. Accessed: 2026-01-29.
- Chen, J., Ge, C., Xie, E., Wu, Y., Yao, L., Ren, X., Wang, Z., Luo, P., Lu, H., and Li, Z. Pixart- $\sigma$ : Weak-to-strong training of diffusion transformer for 4k text-to-image generation, 2024b. URL <https://arxiv.org/abs/2403.04692>. arXiv preprint / project page. Accessed: 2026-01-29.
- Colombo, E., Kirschbaum, C., and Raitelli, M. Legibility of texts: The influence of blur. *Lighting Research & Technology*, 19(3):61–71, 1987.
- Cui, C., Sun, T., Lin, M., Gao, T., Zhang, Y., Liu, J., Wang, X., Zhang, Z., Zhou, C., Liu, H., Zhang, Y., Lv, W., Huang, K., Zhang, Y., Zhang, J., Zhang, J., Liu, Y., Yu, D., and Ma, Y. Paddleocr 3.0 technical report, 2025. URL <https://arxiv.org/abs/2507.05595>.
- DeepMind, G. Imagen 4 (imagen 4 fast) — google / deepmind, 2025. URL <https://deepmind.google/models/imagen/>. Model page / announcement. Accessed: 2026-01-29.
- Eyring, L., Karthik, S., Roth, K., Dosovitskiy, A., and Akata, Z. Reno: Enhancing one-step text-to-image models through reward-based noise optimization. *Advances in Neural Information Processing Systems*, 37:125487–125519, 2024.
- Fallah, F., Patel, M., Chatterjee, A., Morariu, V., Baral, C., and Yang, Y. Textinvision: Text and prompt complexity driven visual text generation benchmark. In *Proceedings of the Computer Vision and Pattern Recognition Conference*, pp. 525–534, 2025.
- (FLUX), B. F. L. Flux.1 [dev] (model card), 2026. URL <https://huggingface.co/black-forest-labs/FLUX.1-dev>. Model card. Accessed: 2026-01-29.
- Google. Nano banana pro (gemini 3 pro image), 2025. URL <https://blog.google/innovation-and-ai/products/nano-banana-pro/>. Product blog. Accessed: 2026-01-29.

- Gu, J., Jiang, X., Shi, Z., Tan, H., Zhai, X., Xu, C., Li, W., Shen, Y., Ma, S., Liu, H., Wang, Y., and Guo, J. A survey on llm-as-a-judge. *arXiv preprint arXiv: 2411.15594*, 2024.
- Heusel, M., Ramsauer, H., Unterthiner, T., Nessler, B., and Hochreiter, S. Gans trained by a two time-scale update rule converge to a local nash equilibrium. *Advances in neural information processing systems*, 30, 2017.
- Hu, J., Shen, L., and Sun, G. Squeeze-and-excitation networks. In *Proceedings of the IEEE/CVF Conference on Computer Vision and Pattern Recognition (CVPR)*, pp. 7132–7141, June 2018. doi: 10.1109/CVPR.2018.00745.
- Ideogram. Ideogram 3 (ideogram v3 / v3 turbo), 2025. URL <https://ideogram.ai/features/3.0>. Product / model page. Accessed: 2026-01-29.
- Kirstain, Y., Polyak, A., Singer, U., Matiana, S., Penna, J., and Levy, O. Pick-a-pic: An open dataset of user preferences for text-to-image generation. *Advances in neural information processing systems*, 36:36652–36663, 2023.
- Korotin, A., Selikhanovych, D., and Burnaev, E. Neural optimal transport. *arXiv preprint arXiv:2201.12220*, 2022.
- Labs, B. F. Flux1.1 pro (product / model page), 2024. URL <https://bfl.ai/models/flux-pro>. Vendor model page. Accessed: 2026-01-29.
- Labs, B. F. Flux.2 [max] (model / product page), 2025. URL <https://replicate.com/black-forest-labs/flux-2-max>. Model / API page. Accessed: 2026-01-29.
- Langley, P. Crafting papers on machine learning. In Langley, P. (ed.), *Proceedings of the 17th International Conference on Machine Learning (ICML 2000)*, pp. 1207–1216, Stanford, CA, 2000. Morgan Kaufmann.
- Lee, K., Liu, H., Ryu, M., Watkins, O., Du, Y., Boutilier, C., Abbeel, P., Ghavamzadeh, M., and Gu, S. S. Aligning text-to-image models using human feedback. *arXiv preprint arXiv:2302.12192*, 2023.
- Li, C., Kou, T., Gao, Y., Cao, Y., Sun, W., Zhang, Z., Zhou, Y., Zhang, Z., Zhang, W., Wu, H., et al. Aigiqa-20k: A large database for ai-generated image quality assessment. In *Proceedings of the IEEE/CVF Conference on Computer Vision and Pattern Recognition*, pp. 6327–6336, 2024.
- Li, H., Wang, P., Shen, C., and Zhang, G. Show, attend and read: a simple and strong baseline for irregular text recognition. In *Proceedings of the Thirty-Third AAAI Conference on Artificial Intelligence and Thirty-First Innovative Applications of Artificial Intelligence Conference and Ninth AAAI Symposium on Educational Advances in Artificial Intelligence, AAAI’19/IAAI’19/EAAI’19*. AAAI Press, 2019. ISBN 978-1-57735-809-1. doi: 10.1609/aaai.v33i01.33018610. URL <https://doi.org/10.1609/aaai.v33i01.33018610>.
- Liao, M., Zou, Z., Wan, Z., Yao, C., and Bai, X. Real-time scene text detection with differentiable binarization and adaptive scale fusion. *IEEE transactions on pattern analysis and machine intelligence*, 45(1):919–931, 2022.
- Long, S., Ruan, J., Zhang, W., He, X., Wu, W., and Yao, C. Textsnake: A flexible representation for detecting text of arbitrary shapes. In *Proceedings of the European conference on computer vision (ECCV)*, pp. 20–36, 2018.
- Min, X., Gu, K., Zhai, G., Yang, X., Zhang, W., Le Callet, P., and Chen, C. W. Screen content quality assessment: Overview, benchmark, and beyond. *ACM Computing Surveys (CSUR)*, 54(9):1–36, 2021.
- Mittal, A., Moorthy, A. K., and Bovik, A. C. No-reference image quality assessment in the spatial domain. *IEEE Transactions on image processing*, 21(12):4695–4708, 2012.
- Novita. Novita ai. <https://novita.ai>, 2024. Accessed: 2024-03-01.
- OpenAI. Chatgpt images (image generation) — openai, 2025. URL <https://help.openai.com/en/articles/8932459-creating-images-in-chatgpt>. Docs / feature page. Accessed: 2026-01-29.
- Podell, D., English, Z., Lacey, K., Blattmann, A., Dockhorn, T., Müller, J., Penna, J., and Rombach, R. Sdxl: Improving latent diffusion models for high-fidelity image generation, 2023. URL <https://arxiv.org/abs/2307.01952>. arXiv preprint. Accessed: 2026-01-29.
- Razhigayev, A., Shakhmatov, A., Maltseva, A., Arkhipkin, V., Pavlov, I., Ryabov, I., Kuts, A., Panchenko, A., Kuznetsov, A., and Dimitrov, D. Kandinsky: An improved text-to-image synthesis with image prior and latent diffusion (kandinsky 2), 2023. URL <https://arxiv.org/abs/2310.03502>. arXiv preprint. Accessed: 2026-01-29.
- Salimans, T., Goodfellow, I., Zaremba, W., Cheung, V., Radford, A., and Chen, X. Improved techniques for training gans. *Advances in neural information processing systems*, 29, 2016.
- Sampaio, G. G., Zhang, R., Zhai, S., Gu, J., Susskind, J., Jaitly, N., and Zhang, Y. Typescore: A text fidelity metric for text-to-image generative models. *arXiv preprint arXiv:2411.02437*, 2024.

- Schuhmann, C., Beaumont, R., Vencu, R., Gordon, C., Wightman, R., Cherti, M., Coombes, T., Katta, A., Mullis, C., Wortsman, M., et al. Laion-5b: An open large-scale dataset for training next generation image-text models. *Advances in neural information processing systems*, 35: 25278–25294, 2022.
- Seedream, B. . Seedream 4.5 (bytedance / seedream), 2025. URL <https://byteplus.com/en/product/Seedream>. Product / API page. Accessed: 2026-01-29.
- Shimoda, W., Inoue, N., Haraguchi, D., Mitani, H., Uchida, S., and Yamaguchi, K. Type-r: Automatically retouching typos for text-to-image generation. In *Proceedings of the Computer Vision and Pattern Recognition Conference*, pp. 2745–2754, 2025.
- Talebi, H. and Milanfar, P. Nima: Neural image assessment. *IEEE transactions on image processing*, 27(8): 3998–4011, 2018.
- Tongyi-MAI. Z-image-turbo (tongyi-mai / alibaba), 2025. URL <https://huggingface.co/Tongyi-MAI/Z-Image-Turbo>. Model card / repo. Accessed: 2026-01-29.
- Tuo, Y., Xiang, W., He, J.-Y., Geng, Y., and Xie, X. Anytext: Multilingual visual text generation and editing. *arXiv preprint arXiv:2311.03054*, 2023.
- UC Berkeley. Lmarena. <https://lmarena.ai/leaderboard/text-to-image>, n.d.
- Xiao, S., Wang, Y., Zhou, J., Yuan, H., Xing, X., Yan, R., Li, C., Wang, S., Huang, T., and Liu, Z. Omnigen: Unified image generation, 2024. URL <https://arxiv.org/abs/2409.11340>. arXiv preprint / project repo. Accessed: 2026-01-29.
- Xu, J., Liu, X., Wu, Y., Tong, Y., Li, Q., Ding, M., Tang, J., and Dong, Y. Imagereward: Learning and evaluating human preferences for text-to-image generation. *Advances in Neural Information Processing Systems*, 36: 15903–15935, 2023.
- Yandex. Yandex.tasks. <https://tasks.yandex.com>, n.d. Accessed 20 December 2025.
- Yang, A., Li, A., Yang, B., Zhang, B., Hui, B., Zheng, B., Yu, B., Gao, C., Huang, C., Lv, C., Zheng, C., Liu, D., Zhou, F., Huang, F., Hu, F., Ge, H., Wei, H., Lin, H., Tang, J., and ... Qwen3 technical report. *arXiv preprint arXiv:2505.09388*, 2025. URL <https://arxiv.org/abs/2505.09388>.
- Ye, P. and Doermann, D. Document image quality assessment: A brief survey. In *2013 12th International Conference on Document Analysis and Recognition*, pp. 723–727. IEEE, 2013.
- Ye, X., Du, Y., Tao, Y., and Chen, Z. Textssr: Diffusion-based data synthesis for scene text recognition. In *Proceedings of the IEEE/CVF International Conference on Computer Vision*, pp. 17464–17473, 2025.
- You, Z., Li, Z., Gu, J., Yin, Z., Xue, T., and Dong, C. Depicting beyond scores: Advancing image quality assessment through multi-modal language models. In *European Conference on Computer Vision*, pp. 259–276, 2024.
- You, Z., Cai, X., Gu, J., Xue, T., and Dong, C. Teaching large language models to regress accurate image quality scores using score distribution. In *IEEE/CVF Conference on Computer Vision and Pattern Recognition*, pp. 14483–14494, 2025.
- Zai-Org. Cogview4 (repo / model), 2025. URL <https://github.com/zai-org/CogView4>. Project / model release. Accessed: 2026-01-29.
- Zhang, R., Isola, P., Efros, A. A., Shechtman, E., and Wang, O. The unreasonable effectiveness of deep features as a perceptual metric. In *Proceedings of the IEEE conference on computer vision and pattern recognition*, pp. 586–595, 2018.
- Zhang, T., Wang, X., Tai, Z., Li, L., Chi, J., Tian, J., He, H., and Wang, S. Strict: Stress test of rendering images containing text. *arXiv preprint arXiv:2505.18985*, 2025a.
- Zhang, Z., Kou, T., Wang, S., Li, C., Sun, W., Wang, W., Li, X., Wang, Z., Cao, X., Min, X., et al. Q-eval-100k: Evaluating visual quality and alignment level for text-to-vision content. In *Proceedings of the Computer Vision and Pattern Recognition Conference*, pp. 10621–10631, 2025b.
- Zhipu AI (Z.ai) Model Team. Glm-4.6: Advanced agentic, reasoning, and coding capabilities. Technical description and model release available on Hugging Face and Z.ai documentation, 2025. URL <https://huggingface.co/zai-org/GLM-4.6>. Model repository: <https://huggingface.co/zai-org/GLM-4.6>.
- Zhu, H., Wu, H., Li, Y., Zhang, Z., Chen, B., Zhu, L., Fang, Y., Zhai, G., Lin, W., and Wang, S. Adaptive image quality assessment via teaching large multimodal model to compare. In *The Thirty-eighth Annual Conference on Neural Information Processing Systems*, 2024. URL <https://openreview.net/forum?id=mHtOyh5taj>.
- Zhu, Y., Chen, J., Liang, L., Kuang, Z., Jin, L., and Zhang, W. Fourier contour embedding for arbitrary-shaped text detection. In *Proceedings of the IEEE/CVF conference on computer vision and pattern recognition*, pp. 3123–3131, 2021.

## Appendix Contents

Implementation Details .....	12
ANTIQA Architecture Specifications .....	12
Training Recipe .....	12
OCR Confidence Mapping to MOS Scale .....	13
Image-Level Aggregation Details and Pooling Ablations .....	13
Speed and Compute Measurement Protocol .....	14
VLM Judging Protocol (Prompting and Score Parsing) .....	14
Text Region Detection and Crop Preprocessing (TIQA-Crops and TIQA-Images) .....	15
Extended Results .....	15
Downstream task: predicting failures for OCR and VLM models .....	15
Decomposing the correlation between overall quality (OQ-MOS) and text quality (TQ-MOS) .....	16
Per-Generator/Per-Prompt Breakdown on TIQA-Images .....	17
ANTIQA ablations .....	18
Analysis of VLM Behavior for Different Prompts .....	18
Extended Dataset Details .....	18
TIQA-Images Prompt List .....	18
Generator List and Versioning .....	19
Subjective Study Protocol and Statistics .....	20

## A. Implementation Details

### A.1. ANTIQA Architecture Specifications

ANTIQA maps an input image batch  $I \in \mathbb{R}^{B \times C \times H \times W}$  ( $C=2$ ) to a scalar quality score per sample. The backbone is a 3-stage CNN with residual blocks, GroupNorm, and SE gating, followed by multi-scale grid pooling and an MLP regressor.

**Backbone.** A stem applies  $\text{Conv}_{3 \times 3}(C \rightarrow 64) + \text{GN} + \text{ReLU}$ . Stage 1 uses two residual blocks at 64 channels, followed by downsampling to 128 channels; Stage 2 uses two residual blocks at 128 channels, followed by downsampling to 256 channels; Stage 3 uses two residual blocks at 256 channels. After each stage output  $X_s$ , an SE block is applied:  $z = \text{GAP}(X_s)$ ,  $w = \sigma(W_2 \text{ReLU}(W_1 z))$ , and  $\text{SE}(X_s) = X_s \odot w$  (reduction  $r=16$ ).

**Multi-scale pooling and projection.** For each scale  $s \in \{0, 1, 2\}$  with channels  $C_s \in \{64, 128, 256\}$ , adaptive pooling to a  $G \times G$  grid ( $\text{grid\_size}=2$ ) is computed:  $A_s = \text{AvgPool}_{G \times G}(X_s)$  and  $M_s = \text{MaxPool}_{G \times G}(X_s)$ . After flattening and concatenation,  $p_s = [\text{vec}(A_s); \text{vec}(M_s)] \in \mathbb{R}^{B \times (2C_s G^2)}$ , then a linear projection yields  $f_s = W_s p_s + b_s \in \mathbb{R}^{B \times 64}$ . The final visual descriptor is  $f = [f_0; f_1; f_2] \in \mathbb{R}^{B \times 192}$ .

An MLP regressor maps  $f$  to a scalar:  $192 \rightarrow 256 \rightarrow 128 \rightarrow 32 \rightarrow 1$  with ReLU and dropout, returning  $\hat{y} \in \mathbb{R}^B$ .

### A.2. Training Recipe

We train the model in two stages: (i) pretraining on an OCR-confidence proxy target and (ii) fine-tuning on human Mean Opinion Scores (MOS). In both stages, we minimize a weighted combination of a regression loss and a ranking loss:

$$\mathcal{L} = \alpha \mathcal{L}_{\text{mse}} + (1 - \alpha) \mathcal{L}_{\text{rank}}; \alpha = 0.5. \quad (5)$$

We optimize with AdamW using learning rate  $10^{-4}$ , weight decay  $w = 0.5$ , batch size  $B = 4$ , and train for  $E_{\text{pre}} = 20$  epochs (pretraining) and  $E_{\text{ft}} = 20$  epochs (fine-tuning).

We use a step schedule with step size  $S = 5$  epochs and decay factor  $\gamma = 0.5$ .

All experiments are run with random seed 42. Training is performed on NVIDIA A100 GPU with total compute of 35 GPU-hours.

Table 3. Effect of aggregation on image-level correlation. Correlations were computed on the whole TIQA-Images dataset against TQ-MOS (text-only quality score). Best score is bolded. Higher is better ( $\uparrow$ ).

Aggregation	TOPIQ		PaddleOCR		Qwen3		ANTIQA		Average	
	PLCC $\uparrow$	SROCC $\uparrow$								
Simple area-weighted mean	0.493	0.470	0.761	0.787	0.489	0.510	0.842	0.837	0.646	0.651
Area $^\alpha$ -weighted mean	<b>0.512</b>	<b>0.483</b>	<b>0.780</b>	<b>0.792</b>	<b>0.503</b>	<b>0.527</b>	<b>0.844</b>	<b>0.841</b>	<b>0.660</b>	<b>0.661</b>
Coverage-aware blend	0.241	0.204	0.476	0.455	0.213	0.221	0.511	0.517	0.360	0.349
Softmin (log-sum-exp)	0.485	0.466	0.749	0.771	0.463	0.490	0.819	0.813	0.629	0.635
Bottom- $k$ mean	0.461	0.459	0.712	0.756	0.448	0.475	0.793	0.802	0.604	0.623
Power mean	0.479	0.460	0.738	0.765	0.451	0.477	0.806	0.802	0.619	0.626

### A.3. OCR Confidence Mapping to MOS Scale

We evaluated several candidate regression families to determine an appropriate parametric mapping from PaddleOCR confidence scores to subjective ratings (MOS). The candidates included random forest, a four-parameter logistic model, a five-parameter logistic model, support-vector regression with an RBF kernel, and ridge regression. Model selection showed that the five-parameter logistic provided the best fit to human judgments, in terms of correlations with MOS estimates on 10,000 crops from TIQA-Crops. Following this selection we fit the chosen parametric form within our neural optimal transport framework to obtain a final mapping from PaddleOCR confidence scores (interval  $[0, 1]$ ) to MOS (interval  $[0, 5]$ ).

The initial correlations between raw PaddleOCR confidence scores and MOS scores were the following: PLCC = 0.7734 and SROCC = 0.7857. After mapping, they improved slightly to values: PLCC = 0.8054 and SROCC = 0.7935. Then, mapped scores for 110,000 crops were used at the pretrain stage of the proposed ANTIQA model.

### A.4. Image-Level Aggregation Details and Pooling Ablations

Given an image, we detect  $N$  text crops. Each crop  $i$  has a predicted quality score  $s_i \in [0, 5]$  and an area fraction  $a_i \in (0, 1]$  relative to the full image. Total text coverage is  $A = \sum_{i=1}^N a_i$ .

We define normalized area weights as  $w_i(\alpha) = \frac{a_i^\alpha}{\sum_{j=1}^N a_j^\alpha}$  with  $\alpha \geq 0$ . Unless otherwise noted, methods below use  $w_i(\alpha)$ . Typical settings:  $\alpha = 1$  (simple area weighting),  $\alpha = 0.5$  (damped dominance),  $\alpha = 0$  (uniform).

**List of pooling techniques.** We map  $\{(s_i, a_i)\}_{i=1}^N \mapsto S_{\text{img}}$  using one of the following.

- Simple area-weighted mean.**  $S_{\text{area}} = \sum_{i=1}^N w_i(1) s_i$ . (Parameter: none; fixed  $\alpha = 1$ .)
- Area $^\alpha$ -weighted mean.**  $S_{\text{mean}}(\alpha) = \sum_{i=1}^N w_i(\alpha) s_i$ . (Parameter:  $\alpha$ ; default  $\alpha = 0.5$ .)
- Coverage-aware blend (prior + crop aggregate).**  $S_{\text{cov}} = (1 - \beta(A)) s_0 + \beta(A) S_{\text{mean}}(\alpha)$  with  $\beta(A) = 1 - e^{-A/A_0}$ . (Parameters: prior  $s_0$ , coverage scale  $A_0$ , and  $\alpha$ ; defaults  $s_0 \in \{10, 5\}$ ,  $A_0 = 0.03$ ,  $\alpha = 0.5$ .)
- Softmin (log-sum-exp).**  $S_{\text{softmin}}(\tau, \alpha) = -\tau \log\left(\sum_{i=1}^N w_i(\alpha) e^{-s_i/\tau}\right)$ ,  $\tau > 0$ . (Parameters:  $\tau$ ,  $\alpha$ ; defaults  $\tau = 1.0$ ,  $\alpha = 0.5$ .)
- Bottom- $k$  mean.** Let  $s_{(1)} \leq \dots \leq s_{(N)}$  be sorted scores. Then  $S_{\text{botk}}(k) = \frac{1}{k} \sum_{i=1}^k s_{(i)}$ . (Parameter:  $k$  or  $k = \lceil \text{frac} \cdot N \rceil$ ; defaults  $\text{frac} = 0.2$  or  $k \in \{1, 2\}$  for small  $N$ .)
- Power mean (generalized mean).**  $S_{\text{pm}}(p, \alpha) = \left(\sum_{i=1}^N w_i(\alpha) \tilde{s}_i^p\right)^{1/p}$  with  $\tilde{s}_i = \max(s_i, \varepsilon)$ . (Parameters:  $p \neq 0$ ,  $\varepsilon > 0$ ,  $\alpha$ ; defaults  $p = -2$ ,  $\varepsilon = 10^{-3}$ ,  $\alpha = 0.5$ .)

If  $N = 0$ , we either return the prior  $s_0$  (when using the coverage-aware formulation) or mark the sample as “no text detected” and exclude it from text-quality evaluation, depending on protocol.

Table 3 shows that area<sup>( $\alpha$ )</sup>-weighted mean pooling is the clear winner across all four OCR/TIQA pipelines, achieving the best average correlation with TQ-MOS (PLCC 0.660 / SROCC 0.661) and consistently topping each individual model (e.g., PaddleOCR 0.780/0.792, ANTIQA 0.844/0.841). Relative to simple area-weighting, the gains are modest but systematic, suggesting that damping the dominance of very large crops (via ( $\alpha \leq 1$ )) better matches human text-quality judgments by letting multiple regions contribute. In contrast, methods that explicitly emphasize worst-case regions (softmin, bottom-(k), power mean with negative (p)) generally reduce correlation, indicating that penalizing a few low-quality crops overstates their impact at the image level. The coverage-aware blend collapses to much lower correlations, implying that injecting a global prior based on total text coverage is misaligned with a \*text-only\* MOS target (and likely dilutes signal when text is present). Overall, simple weighted averaging is robust, but area<sup>( $\alpha$ )</sup> pooling provides the most reliable improvement, making it the best default aggregator.

### A.5. Speed and Compute Measurement Protocol

The FPS rate for the ANTIQA (proposed), PaddleOCR, SAR, and TOPIQ models was measured by running each model 500 times on the same crop with a resolution of  $256 \times 256$  followed by taking the minimum time. The execution time of Qwen3 and GLM 4.6 was calculated based on 50 requests to the service API novita.ai (Novita, 2024) with the prompt to evaluate the same  $256 \times 256$  crop. However, the measured time includes not only the model calculations themselves, but also additional operations, we consider them negligible.

FLOPs for ANTIQA were estimated per-forward using off-the-shelf profiler on the same input crop (batch size 1, same  $256 \times 256$  resolution).

### A.6. VLM Judging Protocol (Prompting and Score Parsing)

Qwen3 (Yang et al., 2025) and GLM 4.6 (Zhipu AI (Z.ai) Model Team, 2025) were accessed via the API of the service novita.ai (Novita, 2024). All the crops from TIQA-Crops and images from TIQA-Images were uploaded to the Internet in order to enable VLM to view and download them. Prompts are presented below:

**Prompt for TIQA-Crops test crops:** "Imagine that you are an OCR model and that you are looking at the quality of the text in the picture. Your task is to produce a real number from 0 to 5, which will represent the quality of the text in the picture in terms of artifacts. In real OCR models, this number is called ocr\_score or confidence\_score. You can use fractional values like 4.33 or 1.23."

**Prompt for TIQA-Images:** "You will see images generated by artificial intelligence, which often look high-quality, but may contain subtle artifacts in the text. Your task is to evaluate ONLY the quality of the text in the image. What NOT to consider: any content of image other than text, semantic correctness of the text, realistic and naturalness, sharpness, noise, and other processing defects. Take into account ONLY visible defects in the text, non-existent letters, and text distortions, as they affect the overall impression. Score 0: Very low quality. Score 1: Strong distortion of the text throughout the image, a lot of interference. Score 2: Text distortion is very noticeable. Score 3: Some defects in the text are noticeable on closer inspection. Score 4: Almost all the text looks perfect, there are minor defects. Score 5: The image does not contain any text defects, the whole text is perfectly readable.

You can use fractional values such as 4.33 or 1.23. In your answer, give only one real number."

Settings such as temperature and max\_tokens, were not changed and those provided by the novita.ai (Novita, 2024) were used, and the values were set to temperature = 1.0, max\_tokens = the size of the context window.

**A.7. Text Region Detection and Crop Preprocessing (TIQA-Crops and TIQA-Images)**

Before evaluating the text crops, it is necessary to detect text regions. In the course of our research, it turned out that the detection module of PP-OCrv5 (Cui et al., 2025) is sufficiently capable for this task. Empirically, we eliminated other detectors (for example, FCENet (Zhu et al., 2021), TextSnake (Long et al., 2018), DBNet++ (Liao et al., 2022)) (see Figure 5).

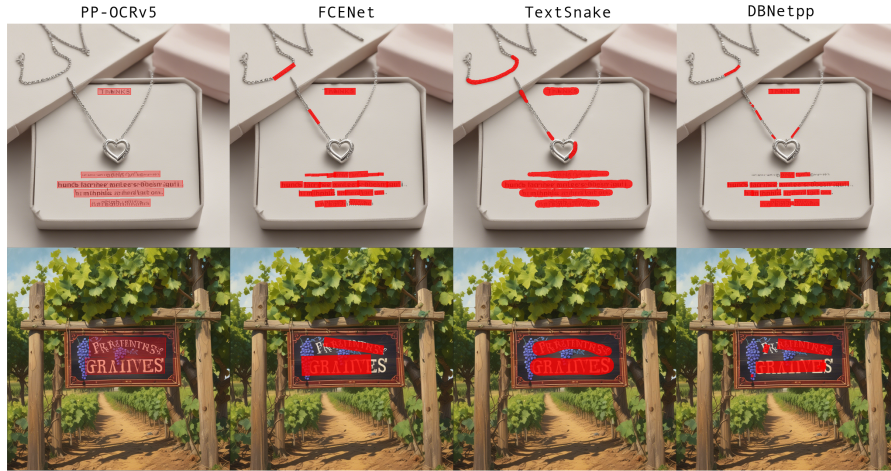


Figure 5. Visualization of crop detections with artifacts from different detectors. The red areas visualize the text detected by the detector.

However the PP-OCrv5 detector (Cui et al., 2025) sometimes detects text where it clearly does not exist. To reduce the number of fake crops in datasets, at the detection stage we additionally ran the OCR module of PP-OCrv5 (Cui et al., 2025) on each detected crop and examined the confidence: if it was below threshold of 0.2, the crop was discarded. We also filtered out image crops smaller than 20 pixels in height. After detection, each crop is rectified to a horizontal orientation using a perspective transform.

**B. Extended Results**

**B.1. Downstream task: predicting failures for OCR and VLM models**

Another downstream task for which potential TIQA models are suitable is the prediction of recognition errors and hallucinations produced by OCR and VLM systems. To demonstrate this, we ran a controlled experiment and analysis pipeline.

**Overview.** we first collected clean text crops from generated images, then used OCR and VLMs to obtain reliable baseline recognized texts, discarding low-confidence samples. Each crop was then progressively degraded using a six-stage distortion pipeline. OCR, VLM, ANTIQA, and TOPIQ were applied to all distorted versions in order to obtain texts, confidences and quality predictions. Finally, we measured recognition errors using normalized Levenshtein similarity and analyzed how these errors correlate with OCR/VLM confidence scores and ANTIQA/TOPIQ predictions. High correlation indicates that TIQA scores effectively capture image and text degradation relevant to OCR and VLM hallucinations.

We denote the  $k$ -th corrupted version of crop  $n$  by  $c_{n,k}$  (with  $k = 1, \dots, 6$ ). Let  $ref_n$  be the ground-truth text (from the clean crop). Denote OCR/VLM recognized text on  $c_{n,k}$  by  $hyp_{n,k}$ . We define the normalized Levenshtein error

$$nsim_{n,k} = 1 - \frac{d_{lev}(ref_n, hyp_{n,k})}{\max\{|ref_n|, |hyp_{n,k}|, 1\}}$$

where  $d_{lev}(\cdot, \cdot)$  is the Levenshtein edit distance;  $nsim_{n,k} \in [0, 1]$  with 1 meaning perfect match.

**Distortion of crops.** A modified TextSSR pipeline was used to generate distorted crops. Initially, the TextSSR (Ye et al., 2025) pipeline uses areas of text cut out of images as conditioning, as well as rendered glyphs on a white background.

We took these rendered glyphs at inference time and distorted them in two ways: by applying Gaussian blur with different radii and by applying JPEG compression with different quality settings. Intuitively, this can be described as “blurring the eyes” of the diffusion model, which leads to poorer-quality text generation. We also ran the TextSSR pipeline twice and three times in succession, replacing the original clean crops with the generated ones and thereby degrading the input data for the next iteration. An example of gradual distortion in a Figure 6.



Figure 6. An example of gradual crop distortion, from left to right.

**Results.** Figure 7 shows PLCC and SROCC correlations for all tested models. The proposed ANTIQA model is predominantly ahead, especially for the task of detecting Qwen3 hallucination (the left figure). PaddleOCR and GLM 4.6 are not far behind, which also perform well, especially in the task of detecting PaddleOCR errors (fourth graph) and detecting GLM 4.6 hallucinations (second graph).

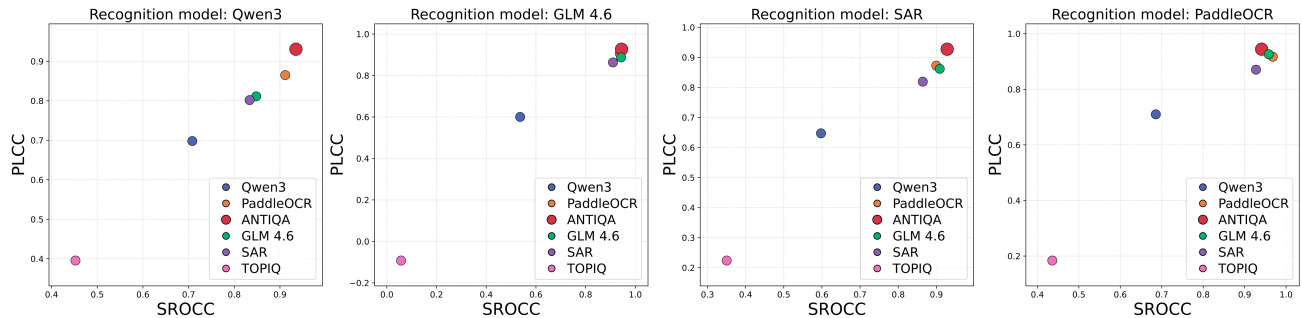


Figure 7. Binned mean normalized Levenshtein similarity as a function of predicted by TIQA models score.

## B.2. Decomposing the correlation between overall quality (OQ-MOS) and text quality (TQ-MOS)

Table 4. Decomposing the correlation between human overall quality (OQ-MOS) and text quality (TQ-MOS) on TIQA-Images. TIQA-Images contains  $P=30$  prompts,  $G=10$  generators, and  $K=5$  seeds per (prompt, generator) pair.

Correlation level	# points	SROCC	Notes
Pooled (all images)	$GPK = 1500$	0.78	As reported in Sec. 6.3
Between generators (means)	$G = 10$	0.98	Correlate $OQ_g$ vs. $TQ_g$
Within (prompt, generator)	$S = 300$	$0.51 \pm 0.43$	Mean $\pm$ std of $\rho_{g,p}$ over $K=5$ seeds
(median)	$S = 300$	0.59	Median of $\rho_{g,p}$

TIQA-Images contains generations from  $G = 10$  text-to-image generators evaluated on  $P = 30$  prompts, with  $K = 5$  random seeds per (generator, prompt) pair, for a total of  $GPK = 1500$  images. Each image  $(g, p, k)$  has two human mean-opinion scores (MOS): overall image quality  $OQ_{g,p,k}$  (OQ-MOS) and text rendering quality  $TQ_{g,p,k}$  (TQ-MOS). We report Pearson linear correlation (PLCC) and Spearman rank correlation (SROCC) as measures of association. A pooled correlation computed over all images can be inflated by between-generator differences. If some generators are systematically better at both rendering text and producing overall high-quality images, the pooled correlation may appear large even if, within a fixed generator and prompt, seed-to-seed variation in text quality is unrelated to seed-to-seed variation in overall quality. To address this concern, we compute correlations at multiple levels of control (Table 4).

We first compute the association between overall quality and text quality over all images:

$$\rho_{\text{all}} = \text{corr}(\{OQ_{g,p,k}\}, \{TQ_{g,p,k}\}),$$

where  $\text{corr}(\cdot, \cdot)$  is either PLCC or SROCC and the sets range over all  $g \in \{1, \dots, G\}$ ,  $p \in \{1, \dots, P\}$ , and  $k \in \{1, \dots, K\}$ . This yields the pooled OQ-MOS-TQ-MOS correlation reported in the main text (SROCC  $\approx 0.78$ ).

To isolate how much of the association is explained by systematic differences between generators, we average scores within each generator across all prompts and seeds:

$$\overline{OQ}_g = \frac{1}{PK} \sum_{p=1}^P \sum_{k=1}^K OQ_{g,p,k}, \quad \overline{TQ}_g = \frac{1}{PK} \sum_{p=1}^P \sum_{k=1}^K TQ_{g,p,k}.$$

We then compute the correlation across the  $G = 10$  generator-level points:

$$\rho_{\text{gen}} = \text{corr}(\{\overline{OQ}_g\}_{g=1}^G, \{\overline{TQ}_g\}_{g=1}^G).$$

Empirically, this between-generator association is extremely high (PLCC=0.96, SROCC=0.98), indicating that generators that render text better are almost always judged better overall on these text-heavy prompts.

To test whether the association persists when generator and prompt are held fixed, we compute a within-pair Spearman correlation across the  $K = 5$  seeded samples for each (generator, prompt) pair:

$$\rho_{g,p} = \text{SROCC}(\{OQ_{g,p,k}\}_{k=1}^K, \{TQ_{g,p,k}\}_{k=1}^K).$$

This produces  $S = GP = 300$  within-pair correlations. We summarize the distribution of  $\rho_{g,p}$  by reporting its mean, standard deviation, and median across the 300 pairs. Empirically, we observe a strongly positive within-pair association (mean SROCC=0.51, std=0.43, median=0.59), showing that even for the same generator on the same prompt, seeds that yield better text are typically also rated better overall. Overall, the near-perfect between-generator correlation shows that text quality is a major axis separating systems on text-heavy prompts, while the strong within-(generator, prompt) correlations show that the association is not merely an artifact of comparing different generators. Instead, seed-level improvements in text rendering quality tend to coincide with seed-level improvements in overall perceived quality in this regime (Table 4).

### B.3. Per-Generator/Per-Prompt Breakdown on TIQA-Images

The Figure 8 decomposes performance into expected accuracy and sampling reliability by plotting the mean score (colour) and the standard deviation across five seed generations (marker size) for each prompt. Across prompts, several models attain similarly strong means, but their seed-level dispersion differs markedly: Seedream 4.5 and Z-Image-Turbo frequently combine high averages with larger variability, while SDXL is consistently lower on average yet comparatively tight. This gap matters for real use, since a high mean with high seed variance implies a non-trivial chance of poor single-shot outputs and a greater need for resampling. These results motivate reporting seed dispersion alongside mean, and adopting risk-aware summaries such as lower quantiles or pass rates at a fixed quality threshold to better reflect deployment-facing robustness.

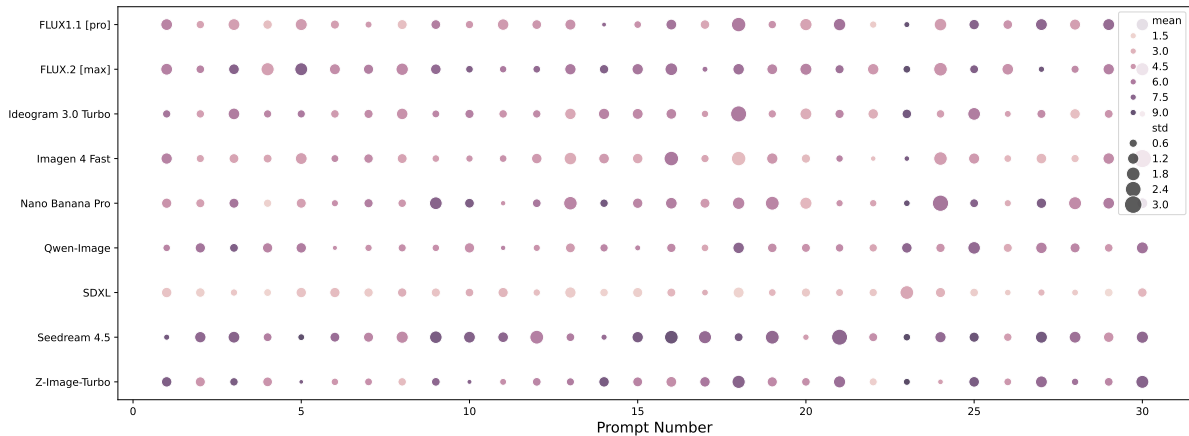


Figure 8. Prompt and seed dependencies across text-to-image models ON TIQA-Images. Colour encodes the mean TQ-MOS per prompt, and marker size encodes the standard deviation across five seed generations, capturing within-prompt sampling variability.

#### B.4. ANTIQA ablations

Table 5 confirms that ANTIQA’s main components materially affect performance on TIQA-Crops. The full model reaches 0.942 PLCC / 0.935 SROCC, while removing OCR-confidence pretraining causes a clear drop to 0.887 / 0.881, highlighting the value of leveraging the 110k proxy-labeled crops before finetuning on the 10k MOS set. Architecturally, strip convolutions are crucial: replacing the proposed strip conv blocks with standard convolutions substantially degrades performance to 0.890 / 0.876, consistent with the need for directionally-aware modeling of text-like structures. Removing multi-scale feature extraction yields the largest drop (0.834 / 0.836), further indicating that text artifacts must be captured across scales.

Table 5. ANTIQA ablations on TIQA-Crops. Full-model numbers are from Table 1 in the paper; the provided PDF does not include the ablation-result values.

ANTIQA ablation (TIQA-Crops test)	PLCC	SROCC
Full ANTIQA (proposed)	0.942	0.935
w/o OCR-confidence <b>pretraining</b> on 110k proxy-labeled crops	0.887	0.881
w/o <b>neural optimal transport</b> mapping (use raw OCR confidence)	0.933	0.927
w/o <b>Sobel edge-map</b> input (grayscale only)	0.920	0.923
w/o <b>strip</b> ( $1 \times k, k \times 1$ ) <b>conv</b> blocks (use standard conv)	0.890	0.876
w/o <b>SE</b> channel gating	0.905	0.908
w/o <b>multi-scale</b> feature extraction (single-scale backbone)	0.834	0.836
w/o <b>avg+max</b> in APB (avg-only)	0.895	0.901
w/o <b>avg+max</b> in APB (max-only)	0.903	0.904

#### B.5. Analysis of VLM Behavior for Different Prompts

We design a controlled prompt-sensitivity study using four variants of the same base prompt, each adding a progressively larger amount of task-specific detail. For evaluation, we sample 60 images from TIQA-Images at random and run Qwen3 three independent times per prompt–image pair to account for generation stochasticity. Results show that performance varies noticeably across prompt variants, indicating that Qwen3 is highly prompt-dependent: changes in wording and the level of instruction detail can lead to non-trivial shifts in correlation with MOS. This further underscores the unreliability of current VLM-based evaluation: despite identical inputs, performance can fluctuate substantially with prompt edits and across repeated runs, indicating limited robustness and weak reproducibility.

Table 6. Correlation of Qwen3 with MOS scores using different prompts on 60 images.

Prompt	TQ–MOS		OQ–MOS	
	PLCC	SROCC	PLCC	SROCC
1	0.6785	0.6912	0.6628	0.6866
2	0.4342	0.4983	0.4772	0.5392
3	0.6749	0.6505	0.7043	0.7066
4	0.5683	0.6004	0.5706	0.5708

## C. Extended Dataset Details

### C.1. TIQA-Images Prompt List (Text-Heavy Prompts)

Here we show a couple examples out of 30 prompts created for TIQA-Images dataset:

**Prompt 1.** A photorealistic airport departures board, wide angle. The board has 30+ rows with small text, columns, and mixed alphanumeric codes. Include slight motion blur from people passing, but the board itself should remain readable. Columns:

Time — Flight — Destination — Gate — Status

Include these exact rows somewhere:

06:45 KL 1023 AMSTERDAM D12 BOARDING

09:10 QR 274 DOHA B07 ON TIME

12:30 TK 1952 ISTANBUL C03 LAST CALL

18:05 EK 148 DUBAI A19 DELAYED 45 MIN

Add a ticker line at bottom in tiny text:

Security notice: do not leave baggage unattended.

**Prompt 2.** A TV karaoke screen in a dim room. The screen shows large lyrics and a second line of smaller subtitles, plus a dense list of upcoming lines in tiny text on the side. Add mild moiré from filming a screen.

Lyrics (large):

WE KEEP RUNNING THROUGH THE NIGHT

UNTIL THE MORNING LIGHT

Small subtitle line:

(sing along)

Include a tiny song code:

Track ID: K-10492

**Prompt 3.** A clean comic page with multiple panels. Each panel has speech bubbles with readable text, plus tiny sound effects and small panel captions. Some speech bubbles are curved.

Include these exact bubble lines:

We can't trust the first render.

Zoom in—look at the kerning!

Why is every third letter wrong?

Add tiny sound effect text:

buzz\* \*click\*

Full list of prompts will be released alongside the dataset.

### C.2. Generator List and Versioning

The models used to generate images for both datasets are shown in the Table 7. All settings and initial parameters were set to default.

Table 7. Generators used for TIQA datasets

#	TIQA-Crops	TIQA-Images
1	PixArt Alpha (Chen et al., 2023b)	GPT Image 1.5 (OpenAI, 2025)
2	SD 3.5 Large Turbo (AI, 2024b)	FLUX1.1 [pro] (Labs, 2024)
3	SD 2.1 (AI, 2022b)	FLUX.2 [max] (Labs, 2025)
4	PixArt Sigma (Chen et al., 2024b)	Seedream 4.5 (Seedream, 2025)
5	SD 3.5 Medium (AI, 2024c)	Ideogram 3.0 Turbo (Ideogram, 2025)
6	Kandinsky 2 (Razzhigaev et al., 2023)	Imagen 4 Fast (DeepMind, 2025)
7	Omnigen (Xiao et al., 2024)	Z-Image-Turbo (Tongyi-MAI, 2025)
8	SD 3 Medium (AI, 2024d)	Nano Banana Pro (Google, 2025)
9	SD 3.5 Large (AI, 2024a)	Qwen-Image (Alibaba, 2025)
10	DeepFloyd IF (AI, 2022a)	SDXL (Podell et al., 2023)
11	FLUX.1 Dev (, FLUX)	
12	CogView4 (Zai-Org, 2025)	

C.3. Examples

Examples of images for the TIQA-Images dataset are presented in Figure 12 (the whole generated images) and Figure 13 (text-only variants). For the latter, we detected text-regions and fill the rest of the frame with plain white. TIQA-Crops examples in Figure 9



Figure 9. TIQA-Crops examples

D. Human Study Protocol

D.1. Participants’ ability to separately visual quality from semantics

To isolate semantic plausibility from rendering artifacts, we generate text crops with an identical prompt template, layout, and typography, varying only the target string: a real word (`world`), an anagram with identical characters (`wrodl`), and a random nonword of the same length (`wuzxh`). We use 5 text-to-image models and generate 5 images per model for each prompt, yielding diverse renderings. Then, we collect 1–5 MOS for visual text quality using the exact same protocol as TIQA-Crops (same instructions, exam, etc.).

We focus on an OCR-correct subset to control for fatal rendering errors: a crop is OCR-correct if an external recognizer returns exactly the target string. On this subset, we compare MOS distributions across strings. Figure 10 shows the MOS distributions for each prompt variant. The distributions largely overlap, with similar means and ranges, suggesting that lexical plausibility has limited effect on the visual text-quality MOS when using this subjective study protocol.

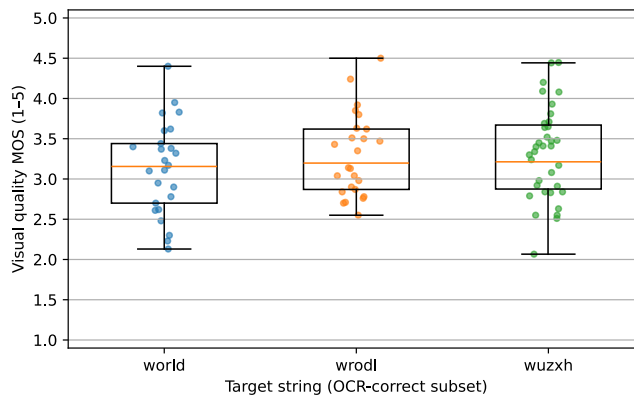


Figure 10. MOS distributions (1–5) for three target strings on the OCR-correct subset (exact transcript match). Similar distributions across a real word, an anagram, and a nonword indicate limited sensitivity of visual-quality ratings to lexical plausibility when rendering is correct.

### D.2. Qualification Exam and Quality Control

Before starting the markup, Yandex.Tasks platform (Yandex, n.d.) users had to pass an exam that tested their understanding of the instructions. For the TIQA-Crops exam there were 10 demonstration crops, of which at least 8 had to be marked correctly; for the TIQA-Images exam there were 4 images, of which at least 2 had to be marked correctly.

The markup was carried out in batches, and for both datasets a user’s answers within a batch were accepted only if they correctly answered one of the quality-control questions that were mixed into each batch.

### D.3. Annotation Statistics and MOS Computation

Each image was independently rated by 50 human raters. We report Mean Opinion Score (MOS) as a 10% trimmed mean: for each image, we discard the lowest 5% and highest 5% of ratings (i.e., the 5 lowest and 5 highest out of 50) and average the remaining 40 ratings. Figure 11 shows distributions of MOS values for TIQA-Images dataset

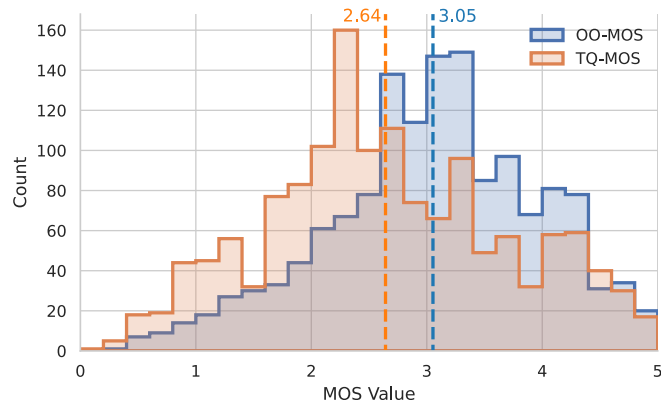


Figure 11. Distribution plot for OQ-MOS and TQ-MOS for TIQA-Images dataset. Vertical dashed lines denote mean values across all images.

### D.4. Rater Instructions

The users of Yandex.Tasks platform (Yandex, n.d.) were fully briefed on the essence of marking up crops for TIQA-Crops dataset and images for TIQA-Images dataset. Full instructions are provided below:



Figure 12. TIQA-Images examples for overall quality

# TIQA: Human-Aligned Text Quality Assessment in Generated Images



Figure 13. TIQA-Images examples for text quality

**Markup instructions for TIQA-Crops dataset:** "Your task is to evaluate the quality of the text in the picture from 0 to 5. The images are derived from generative models, which is why there are artifacts and distortions that need to be taken into account.

Score 0: There is no hint of any text in the picture.

Score 1: confusion: the outline of the text is roughly visible, but it is completely unreadable, it is impossible to identify individual letters. The key difference from a score of 0 is that there is a general outline of the text.

Score 2: the text is still unreadable, but the key difference from score 0 is that individual letters begin to appear.

Score 3: a lot of artifacts: non-existent, stuck, floated or distorted symbols. The key difference from score 2 is that some Latin characters or similar ones are visible. Moreover, these symbols are clearer and more distinguishable.

Score 4: ALMOST ALL the text is perfect and readable, but there are small artifacts. In the illustration, the artifacts are highlighted in red frames. The key difference from score 3 is a lot of readable Latin letters and fewer artifacts.

Score 5: All the text in the picture is READABLE, each letter is in the English alphabet and is clearly visible. A low resolution is acceptable. The key difference from score 4 is the absence of obvious distortions and artifacts.

- There are test tasks, if they are answered incorrectly, the work will not be counted.
- Ignore the meaning and semantics of the text.
- Ignore the resolution of the image. That is, low resolution does not mean poor quality. The purpose of markup is to identify the presence of artifacts, distortions, and confusion.
- Ignore the cropped pieces of other text outside the target label.
- You can select the answer option using the keys "0", "1", etc."

**Markup instructions for TIQA-Images dataset, overall quality:** "You will see images generated by artificial intelligence, which often look high-quality, but may contain unnoticeable artifacts (including in the text). Your task is to evaluate the overall perceived quality of the entire image.

What needs to be considered:

- realistic and natural images
- sharpness, noise, and other processing artifacts
- visible text artifacts are also taken into account because they affect the overall impression.

What NOT to consider:

- the image content itself
- the meaning of the written text

Score 0: Very poor quality (it is difficult or impossible to make out what is shown in the image).

Score 1: Strong artifacts throughout the image, lots of interference.

Score 2: Artifacts are very noticeable (in the main text), but the image looks good enough.

Score 3: Some artifacts are noticeable on closer inspection.

Score 4: Almost the entire picture looks perfect, there are small artifacts that do not affect the overall quality.

Score 5: The image does not contain any artifacts, the entire text is perfectly readable.

- There are test tasks for which the work will not be counted if answered incorrectly.
- Ignore the meaning and semantics of the text
- You can select the answer option using the keys "0", "1", etc."

**Markup instructions for TIQA-Images dataset, text quality:** "You will see images that contain only text areas from the original image. Everything else has been removed and replaced with white. This is intentional.

Your task is to evaluate the visual quality of the text itself, focusing only on the artifacts. This task does NOT concern the content of the text.

Evaluate how visually correct and natural the text looks.: letter shape (absence of "pseudo-letters", deformed glyphs), the integrity of the strokes, interval/kerning sequence, unnatural deformations, blurring, variable thickness

What NOT to consider

- semantics: spelling, grammar, meaning, "does this sentence make sense?", language
- font or styling, if they do not lead to visible distortion
- large white areas (they are expected)
- the overall "composition of the image" (it does not exist by design).

How to view

First, evaluate the image at a normal scale, then zoom in to view the smaller text.

If the text is very small, evaluate whether it looks plausible when zoomed in.

Score 0: very poor quality (it is difficult or impossible to make out what is written on the image)

Score 1: Strong artifacts throughout the image, lots of interference and artifacts

Score 2: The artifacts are highly visible, but the basic inscriptions look good

Score 3: Some artifacts are noticeable on closer inspection, there is a lot of text without artifacts

Score 4: Almost all the text looks perfect, there are small artifacts that do not affect the overall quality

Score 5: The picture does not contain any artifacts, the entire text is perfectly readable

- There are test tasks, if they are answered incorrectly, the work will not be counted
- Ignore the meaning and semantics of the text
- You can select the answer option using the keys "0", "1", etc."